Iran University of Science and Technology

Automotive Science and Engineering

Journal Homepage: ase.iust.ac.ir

ISSN: 2008-9899

Development of an Innovative Flywheel-Based Brake Energy Recovery System for Enhanced Urban Fuel Efficiency in Passenger Cars

Alireza Azarm[1], Mohsen Esfahanian[2*], Hosein Hamidi Rad[3]

[1]Department of Mechanical Engineering, Isfahan University of Technology, Isfahan, Iran

[2]Department of Mechanical Engineering, Isfahan University of Technology, Isfahan, Iran

[3]Department of Mechanical Engineering, Isfahan University of Technology, Isfahan, Iran

ARTICLE INFO

Article history:

Received : 26 Jan 2024

Accepted: 1 May 2024

Published: 6 Jun 2024

Keywords:

Flywheel-based KERS

Brake recovering system

Urban fuel efficiency

Mechanical energy storage

Power transmission and clutch design

Controller optimization

A B S T R A C T

This study presents the design and simulation of a novel flywheel-based kinetic energy recovery system (KERS) intended to enhance fuel efficiency and reduce emissions in urban passenger vehicles, with a specific focus on the Samand car. Conventional KERS technologies typically rely on either electrical or mechanical storage methods to harness energy dissipated during braking. Here, we explore the practicality of a rotating flywheel as an environmentally friendly, cost-effective, and durable mechanical storage alternative, well-suited to the frequent-stop conditions characteristic of urban driving. The system's initial prototype, developed through MATLAB_SIMULINK and ADVISOR simulations, includes optimized design specifications for power transmission and clutch components to ensure efficient energy recovery and release. A detailed analysis of various design parameters highlights their influence on the system's performance, with particular attention to configurations that maximize fuel savings and emission reductions. The simulation results show a significant decrease in fuel consumption for the Samand during urban cycles, achieved using a steel flywheel with an incomplete cone geometry. Suggestions are also provided for refining the controller to improve energy recovery efficiency further, underscoring the system's potential as a viable solution for greener, more efficient vehicle operation in city environments.

1. Introduction

The transportation sector's reliance on fossil fuels has powered economic growth but at a significant environmental cost. Predictions suggest global fossil fuel reserves could be depleted by 2042, driving an urgent need for sustainable energy alternatives in vehicles [1]. This need has intensified efforts to reduce fuel consumption, with Kinetic Energy Recovery Systems (KERS) emerging as a promising solution. KERS captures

*Corresponding Author
Email Address: mesf1964@cc.iut.ac.ir
https://doi.org/10.22068/ase.2024.671

[DOI: 10.22068/ase.2024.671]

braking energy, which would otherwise dissipate as heat, and repurposes it, enhancing fuel efficiency. In urban driving, where frequent stop-and-go patterns are common, braking energy losses can account for a significant portion of fuel consumption, representing a substantial opportunity for energy recovery, particularly in passenger vehicles [2].

Conventional KERS configurations include both electrical and mechanical systems. Electrical KERS, widely used in hybrid and electric vehicles, integrates well with existing electrical systems but faces limitations, including high costs and battery degradation, which can reduce efficiency under high energy demands [3]. By contrast, flywheel-based KERS, a mechanical approach, provides a cost-effective, durable alternative. It offers rapid energy absorption and release while avoiding the degradation issues associated with batteries, making it particularly suitable for urban driving cycles with frequent braking [4]. Boretti (2010) demonstrated that flywheel KERS in compact cars could improve fuel savings by up to 10% over hybrid electric vehicles, capitalizing on rapid energy storage and discharge [5]. Gunatilake et al. (2015) further showed flywheels as an effective solution in conventional vehicles, minimizing battery dependency and associated disposal challenges [6].

Recent research emphasizes the benefits of flywheel KERS in vehicles facing frequent braking demands. Śliwiński (2016) examined design factors such as rotational speed and inertia, confirming flywheels' effectiveness for high-frequency energy recovery [7]. Rakov (2020) further analyzed flywheel optimization in urban settings, demonstrating that well-calibrated systems can enhance energy recovery efficiency in stop-and-go driving conditions [8].

Despite these advantages, few studies have tailored flywheel-based KERS specifically for urban passenger vehicles, leaving a gap in solutions optimized for frequent braking cycles. This study addresses this gap by designing a flywheel-based KERS with a custom controller and transmission configuration suited to the stop-and-go demands of city driving. The methodology details the design process of the KERS and the simulation parameters used to evaluate its performance. Following this, the paper presents the results, analyzing the system's impact on fuel consumption. Finally, it discusses the broader implications of the findings and potential directions for future research.

2. Methodology

The present study aims to design an effective and simple-to-implement energy recovery system and integrate it into a passenger car's conventional powertrain. Initially, the energy capacity for the vehicle is calculated. Then, appropriate materials are selected, and the size and shape of the flywheel are determined. A model is developed and added to the powertrain model in Simulink, and the design parameters are optimized to create a system that is cost-effective, efficient, and easy to implement.

2.1. Energy Tank Design Criteria:

In urban driving cycles, braking typically occurs from speeds between 40 and 60 km/h. For this study, we consider a 1500 kg vehicle (including additional equipment) with an initial braking speed of 60 km/h, yielding a kinetic energy of approximately 208.3 kJ. Assuming an average deceleration to a stop over 5 seconds, we calculate a deceleration rate of -3.33 m/s² and a braking distance of around 14.7 meters.

Potential energy recovery from elevation changes is also considered. For a 6% road slope (3.43°), we calculate a height change of 2.5 meters, yielding an additional potential energy of approximately 36.8 kJ. Summing the kinetic and potential energy, the total available energy during a typical urban braking event is around 245.1 kJ. Applying a 90% mechanical efficiency and 80% rear-axle braking contribution, the effective design target for the flywheel energy capacity is approximately 176.5 kJ.

[DOI: 10.22068/ase.2024.671]

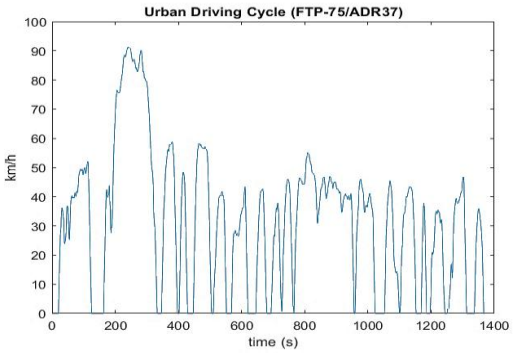

Figure 1. FTP-75 cycle time speed chart [9]

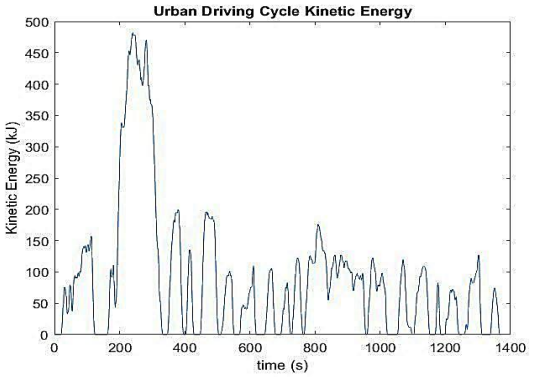

Figure 2. Kinetic energy resulting from FTP-75 cycle for Samand Car cycle for Samand Car [9]

The rotational energy of the flywheel is obtained from $\boldsymbol{E_f = \frac{1}{2} I\omega^2}$ in which "I" is the moment of inertia, ω is the rotation speed and the $\boldsymbol{E_f}$ is the energy stored in the flywheel. By using the rotational energy of the flywheel, its speed reduces. since the speed ratio of the CVT is limited, the lower limit of the flywheel speed cannot be zero, and as a result, the entire rotational energy stored in the flywheel cannot be used. Thus, the usable stored energy is obtained from the following relationship:

$$E_{stored} = \frac{1}{2} I(\omega_{max}^2 - \omega_{min}^2) = \frac{1}{2} I\omega_{max}^2 \left(1 - \frac{\omega_{min}^2}{\omega_{max}^2}\right) \quad (1)$$

The ratio of the upper and lower limits of the efficient rotation speed $\frac{\omega_{min}^2}{\omega_{max}^2}$ depends on the range of CVT coefficients. The lower this ratio, the greater the range of CVT coefficients required in the CVT. By increasing the moment if inertia I, the stored energy will increase directly, however the mass and size will increase. Since the energy stored in the flywheel is related to the square of its rotational speed, by increasing ω, the stored energy will increase much more but the rotational stress will increase too. This fact brings limitations on flywheel design. Composite wheels have less weight, therefore, at a certain rotational speed, less tension will be induced. Modern composite materials have even lower weight and higher resistance which provides the ability to rotate at very high speeds [4]. So, in general, there are three design parameters:

- The resistance of the material that determines the $\boldsymbol{\omega_{max}}$ of the flywheel.

- The maximum rotation speed ($\boldsymbol{\omega_{max}}$) which determines the energy storage capacity of the flywheel.

- The geometry of the flywheel, which determines the specific energy capacity of the system.

Mechanical losses such as heat and aerodynamic drag are significant at high speeds. Placing the flywheel in a vacuum chamber with minimal pressure (or even vacuum) is a widely used as a solution to this problem.

2.2. Operation modes

The operation theory of the system, managed by the control unit, is categorized into three conditions: braking energy recovery mode, acceleration mode, and neutral mode. During the braking energy recovery mode, kinetic energy is absorbed during braking to reduce the vehicle's speed. Initially, the coefficients of the power transmission system (CVT) between the flywheel and the axle are calculated, and their applicability is verified. Subsequently, the rotational speed of the flywheel is assessed within the optimal performance range, and if validated, the flywheel is engaged with the system via the clutch. Concurrently, the CVT coefficients are adjusted to decrease the axle's rotational speed while increasing the flywheel's rotational speed. In this scenario, the default brake system remains on standby, ready to be utilized in instances of heavy braking exceeding the recovery system's capacity.

[DOI: 10.22068/ase.2024.671]

In the acceleration mode, the energy recovered from braking, stored in the rotating flywheel, is redirected to the axle to facilitate vehicle acceleration. Unlike the previous mode, the CVT coefficients are modified to decrease the flywheel's rotational speed while increasing the axle's speed. Once the flywheel's speed reaches the lower limit or the vehicle axle's rotation speed attains the optimal level, the flywheel disengages from the CVT and enters standby mode while the engine remains connected.

During the neutral mode, the flywheel is disconnected from the axle. This mode is activated when either the flywheel's speed or the CVT coefficients fall outside the allowable range, signaling conditions where the flywheel is not engaged with the system.

2.3. Power transmission path

When comes to mechanical KERS, the energy storage (flywheel, accumulator, compressor) acts just like the second power source in hybrid vehicles which can be placed in the parallel formation to the main power supply or they could operate in a series path. It is also recommended to imbed the flywheel axes longitudinally positioned. Parallel configuration is preferred for converting a conventional vehicle to hybrid because of ease of implementation, utilizing components from existing vehicles [10]. So, in this matter, A parallel configuration is chosen for connecting the flywheel system to the power path. The flywheel - CVT set can be placed either before or after the transmission. In both configurations, the power transmission path remains unchanged. The second configuration is the easiest to implement in the power train while in the first configuration, the CVT ratios changes significantly. The advantage of the first configuration is the higher rotational speed before transmission which is closer to the flywheel speed. For this reason, depending on the gear ratio of the transmission, a higher ranged speed ratio CVT should be used in the second configuration.

2.4. Braking control

The main considerations of brake controller used in braking energy recovery system are as follows:

• The energy recovery system must have sufficient capacity to recover braking energy and be implementable.

• The braking system must be reliable in different conditions.

• The amount of recovered energy should be predictable and repeatable for each braking time.

It is assumed a constant power is transmitted to or from the flywheel regardless of the shaft rotational speed. It is clear that higher rotational speed reduces the transmitted torque. To reduce the CVT torque, an increasing gear speed ratio can be used before the CVT. Also, to ensure that the rotational speed of the CVT does not exceed the permissible limit, a decreasing gear speed ratio after the CVT can be used. Applying these two gear ratios will cause negligible power loss. The flywheel rotation speed is calculated as follows:

$$\omega_{flywheel} = \omega_{shaft} \times \eta_{pre} \times \eta_{var} \times \eta_{post} \qquad (2)$$

It is obvious that as the speed of the car increases, the rotation speed of the flywheel and the post-gearing of the CVT decreases to release energy and the torque of these two will increase. However, the pre-gearing and the transmission speeds will increase. Due to the high rotational speed in the post-gearing, the applied torque ratio (η_2) is much lower than the pre- gearing torque ratio (η_1). Also, the power transmission system must have the ability to transmit maximum energy in correct proportions.

A driving cycle is needed to calculate the required power of the system. MATLAB script has been used to calculate that maximum negative energy changes. Flat road and constant deceleration rate (negative acceleration) is assumed. A 90% braking efficiency and 80% rear axle share of the from the total braking is assumed.

$$P_{design} = P_{max} \times 0.8 \times 0.9 = \frac{E_{avail}}{t_{break}} \times 0.8 \times 0.9 \qquad (3)$$

[DOI: 10.22068/ase.2024.671]

By differentiating the kinetic energy of the driving cycle with respect to time, the required power to complete the cycle is obtained and shown in the Figure 3. The negative powers indicate braking and positive powers mean acceleration. The maximum braking power in this cycle for the Samand car is 28.02 kW, and by applying the mechanical efficiency and the rear axle's share of braking, the power capacity becomes 20.17 kW.

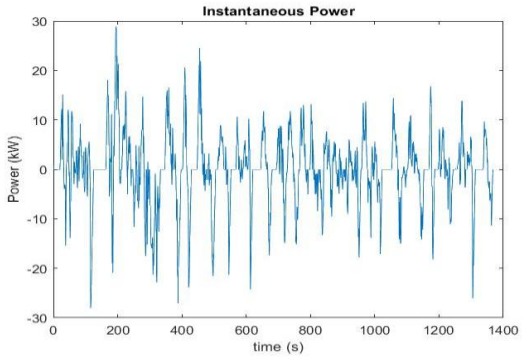

Figure 3. Diagram of the power required to cover the FTP-75 cycle by the Samand vehicle

3. Flywheel design

Low-speed flywheels, typically used in stationary applications, operate with maximum rotational speeds up to 5000 rpm. Achieving high power at low speeds generally involves increasing the mass, but this can lead to high stresses and larger dimensions. In contrast, reducing the mass or radius reduces the moment of inertia, affecting energy storage. Increasing speed enhances energy storage capacity but also results in higher stresses, particularly at the flywheel's periphery. The ratio of the minimum to maximum rotational speed $\frac{\omega_{min}}{\omega_{max}}$ significantly influences the flywheel's efficiency. Recent studies indicate that optimizing this ratio is crucial, with a typical recommended value of around 0.5, which achieves approximately 75% of the theoretical maximum energy capacity [11].

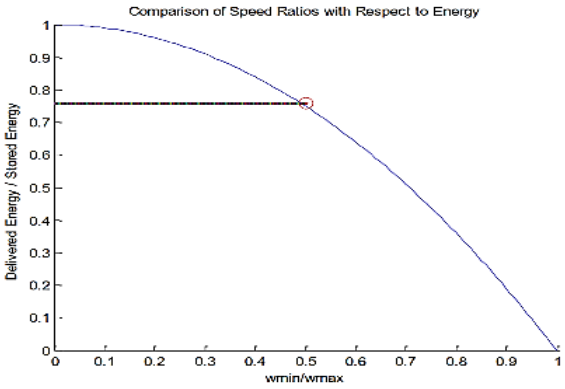

Figure 4. Comparison of flywheel rotation speed ratio according to energy ratio

3.1. Failure analysis

Flywheel design requires a detailed understanding of the failure modes associated with high-speed operation. The most critical factors are the centrifugal forces that induce both radial and tangential stresses. For high-speed flywheels, these stresses need to be carefully estimated to predict the risk of fracture or disintegration [12]. Recent studies suggest using pressure vessel relations to approximate these stresses in flywheels, leading to the following formulas for tangential $\boldsymbol{\sigma_T}$ and radial $\boldsymbol{\sigma_r}$ stresses:

$$\sigma_T = \rho\omega^2\left(\frac{3+\vartheta}{8}\right)\left(r_i^{\,2} + r_o^{\,2} + \frac{r_i^{\,2}r_o^{\,2}}{r^2} - \frac{1+3\vartheta}{3+\vartheta}r^2\right) \quad (4)$$

$$\sigma_r = \rho\omega^2\left(\frac{3+\vartheta}{8}\right)\left(r_i^{\,2} + r_o^{\,2} - \frac{r_i^{\,2}r_o^{\,2}}{r^2} - r^2\right) \quad (5)$$

where ν represents Poisson's ratio, and r_i and r_o are the inner and outer radii of the flywheel, respectively. These formulas highlight the importance of stress analysis in determining the maximum allowable speed and operational limits. As shown in various studies, the tangential stress at the inner radius often dictates failure points due to its magnitude exceeding the material's tensile strength

Both radial and tangential stresses in the distance between the internal radius (r_i) and external radius (r_o) for the flywheel with initial design values have been calculated and shown in Figure 5. It can be seen that at any radius, the

[DOI: 10.22068/ase.2024.671]

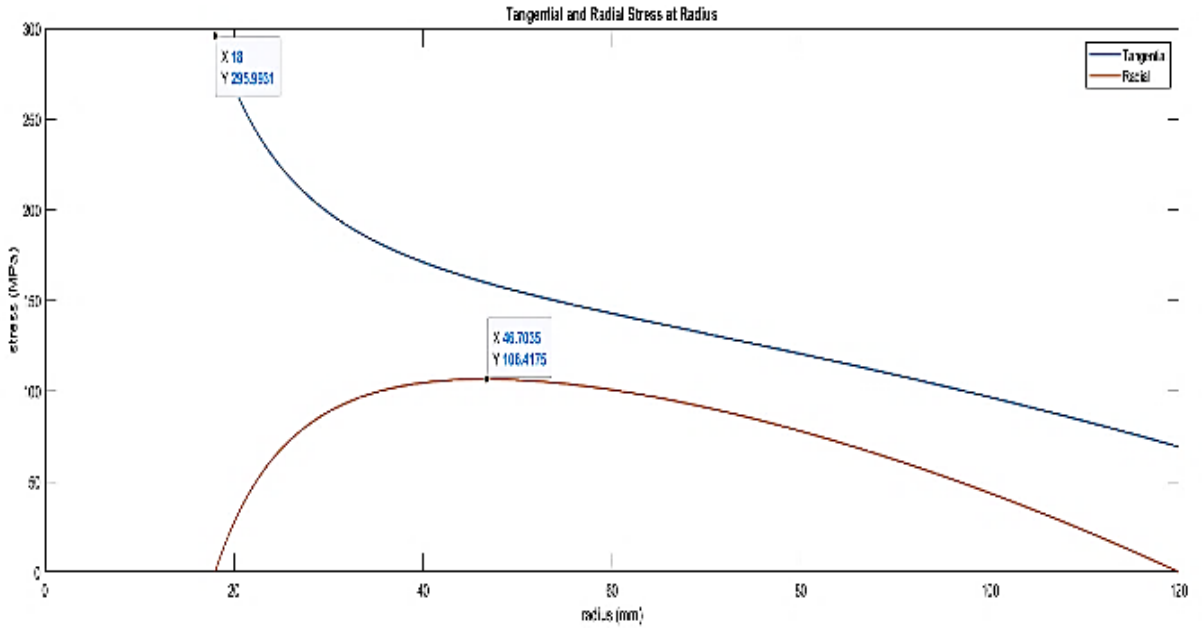

Figure 5. Radial and tangential stress diagram between inner and outer radius

Table1. Shape factor (k) various types of flywheel geometries [16]

Flywheel Geometry	Cross-Section or Pictorial View	Shape k
Constant-Stress Disc (OD -> ∞)		1.0
Modified Constant-Stress Disc (Typical)		.93
Truncated Conical Disc (Typical)		.80
Flat Unpierced Disc		.60
Thin Rim (ID/OD -> 1.0)		.50
Shaped Bar (OD -> ∞)		.50
Rim with Web (Typical)		.40
Single Filament Bar		.33
Flat Pierced Disc		.30

radial stress is lower than the tangential stress and the maximum stress occurs in the radius r_i. It can be concluded that the cause of flywheel failure is the tangential stress in the inner radius.

For each design, ω_{max} determines the energy storage capacity, which is limited by the tensile strength of the flywheel material. The maximum storable energy for a specific geometry is calculated by $E_{max} = KV\sigma$ as long as there is axial symmetry and plane stress. By dividing the density of material (σ), the specific energy (e) is obtained. where in K is the shape factor and V is the volume of flywheel material.

$$e = \frac{E_{max}}{M} = \frac{K\sigma}{\rho} \quad (6)$$

It is obvious that higher shape factor is suitable. In composites, due to the uniaxial strength, usually the shape factors are lower and reaches to maximum of 0.5. In Table 1 shows the shape factor for different geometries. Several geometries are proposed only for composite materials, because they have different strength characteristics (uniaxial in composite materials and also multiaxial resistance in isotropic

[DOI: 10.22068/ase.2024.671]

materials (radial and tangential)). The constant stress flywheel with shape factor of one (called as Laval) is used in [13].

It is suggested to use aluminum cylinders for the center hub because they have multi-axial strength and their light weight has the least impact on the overall design. For thin geometries, a circular disk is needed, which is generally connected to the end hub through a spoke (arm). Adding a spoke or a thin disk is a bit challenging because they have flexibility under load and can cause instability at high speeds. Purohit and Sharma [14] suggested using arms for diameters higher than 60 cm and generally considers rigid rotors as desirable. Arslan [15] suggested a disk with an incomplete conical section is a good choice in terms of shape factor and ease of production.

3.2. **Material and Shape Assumptions**

Different materials can be used in a flywheel depending on the application. Isotropic materials are the most commonly used in flywheels. They are denser compared to anisotropic materials and have lower strength density. Composite materials can have high strength density due to the combination of fibers with different specifications and therefore they can be used for high-speed flywheels. Using composite materials are suitable for reducing the weight of the flywheel, but the difference in Young's modulus of the disk and the embedded metal shaft should be taken into account. However, it will cost more [13]. In an equal situation, isotropic materials are less deformed than anisotropic materials because they have a higher Young's modulus. The most used composites are epoxy reinforced with glass, aramid or carbon fibers. For the same energy capacity, a flywheel made of isotropic materials can occupy less space but have more weight than a composite flywheel.

In common passenger cars, both the specific energy capacity (energy per unit mass) and maximum tolerable rotation speed are crucial for flywheel performance. Composite materials offer a high specific energy capacity, though they can pose design challenges due to a lower shape factor. Our analysis compares energy storage capabilities across various materials based on several assumptions:

- For isotropic materials, an incomplete cone cross-section was modeled, while for anisotropic (composite) materials, a thin ring was assumed, with mass concentrated at the outer radius. These configurations balance weight, structural integrity, and ease of implementation.
- Fatigue stress limits are set to withstand 10^7 cycles, reflecting typical passenger car lifespans and operating conditions in urban settings.

For an ideal composite flywheel, the energy storage at a given radius, R, and speed, ω , is estimated by applying relationships from pressure vessel theory. We apply the formula $\sigma = \rho(r\omega)^2$ to calculate stress, linking energy capacity to rotational speed. The theoretical maximum speed, where tangential stress peaks at the outer rim, informs design limits for safety and performance. Then we have:

$$\frac{\sigma}{\rho} = (r\omega)^2 = v^2 \tag{7}$$

The maximum rotational speed for a composite flywheel with stress concentration in the outer radius of the rim can be calculated from the above equations. For the modeling of the disk made of isotropic materials with constant stress, the following equation is used:

$$\sigma = \frac{\rho v^2}{2\ln\left(\frac{r_0}{w}\right)} \tag{8}$$

From the above equation, speed of the flywheel is obtained:

$$v = \sqrt{\frac{2\sigma\ln\left(\frac{r_0}{w}\right)}{\rho}} \tag{9}$$

Considering two flywheels made of isotropic and anisotropic materials with the same capacity and with constant stress, the velocities should be equated:

[DOI: 10.22068/ase.2024.671]

$$\frac{2\sigma \ln\left(\frac{r_0}{w}\right)}{\rho} = \frac{\sigma}{\rho} \quad (10)$$

And therefore, the ratio of thickness to radius to be used in the design process becomes:

$$\left(\frac{w}{r_0}\right) = 0.607 = KV\sigma \quad (11)$$

The following equation can also be used to calculate the mass of a disk with an incomplete cone section as shown in Figure 6:

$$M = \frac{1}{3} \times \rho\pi(r_1^2 + r_1 r_2 + r_2^2) \times 2h \quad (12)$$

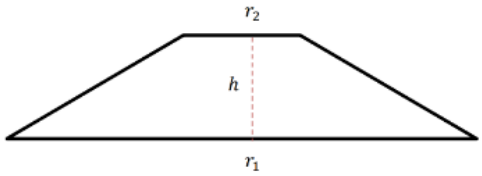

Figure 6. Cross section of incomplete cone flywheel

By performing failure analysis using equations (4) and (5), the outer radius of 12 cm and the inner radius of 1.95 cm are obtained. Using equation (11) a half thickness of 3.6 cm is considered as initial design value for flywheel dimensions as depicted in Figure 7.

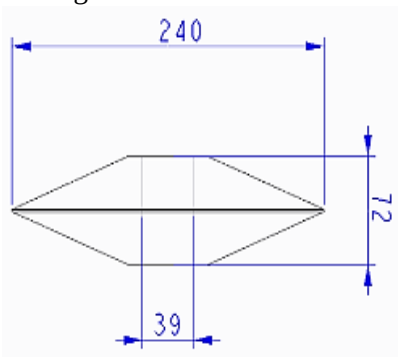

Figure 7. Flywheel dimensions with incomplete cone geometry for initial design

For the ratio $\frac{\omega_{min}}{\omega_{max}} = 0.5$ and the maximum rotational speed, the stored energy is calculated.

$$E_{stored} = \frac{1}{2} IK(\omega_{max}^2 - \omega_{min}^2) = 183 \text{ kJ} \quad (13)$$

Taking into account the comparison between isotropic and anisotropic materials in ref [17], Titanium will be removed from the options due to the excessive price. "Maraging Steel", while being an available and widely used material, is the only isotropic material option that satisfies the size restrictions and has a reasonable manufacturing and implementation cost. Carbon fiber, as an anisotropic material, due to its high specific strength and low density, is a good option if the construction and implementation cost would not be a problem. Carbon fiber flywheels are generally suitable for high-speed applications (60,000 rpm) such as racing cars, and steel flywheels are generally used for low-speed applications such as heavy-duty vehicles.

MATLAB script has been used for the more detailed preliminary design of the flywheel geometry. The energy diagram in terms of outer radius for different ratios ($\frac{r_0}{w}$), made of isotropic material and incomplete cone cylinder geometry, has been obtained and drawn in Figure 8. A safety factor of 1.4 is applied. The higher the ratio ($\frac{r_0}{w}$), the smaller the radius is needed to reach the desired capacity. By intersecting a horizontal line of 183 kJ, the smallest possible radius is 9 cm, with the ratio $\frac{r_0}{w} = 1$ and the largest possible radius is 15 cm with the ratio $\frac{r_0}{w} = 0.2$. For the initial design, a ratio of 0.4 with an outer radius of 12 cm and an inner radius of 1.8 cm are chosen.

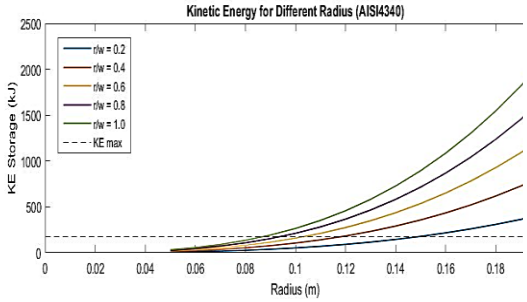

Figure 8. Diagram of energy capacity in terms of radius for isotropic materials with different ratios ($\frac{r_0}{w}$)

The relations given by Juvinall [18] have been used to calculate clutch size with the help of MATLAB. The transmission torque capacity of

[DOI: 10.22068/ase.2024.671]

the clutch is obtained through the following equation, where in p is pressure between plates, f is the coefficient of friction between the plates, N is the number of pages.

$$T = \frac{2}{3}\pi f p (r_o^3 - r_i^3) N \quad (14)$$

Woven metals have been selected as the component of the clutch plates and the safety factor is 4. For the maximum torque, the equation $r_i = \sqrt{\frac{1}{3}} r_o$ is obtained [18]. By rewriting the above equation, the outer radius is obtained:

$$r_o = \sqrt[3]{\frac{T}{\frac{2}{3}(0.805) N p \pi f}} \quad (15)$$

A wet clutch is suitable for high rotational speed and operating frequency. To reduce the drag of clutch plates, increasing the size of the plates has a greater effect than increasing the number of plates [19]. After initial calculations with the help of MATLAB, it was found that if the clutch is placed after the post gearing, its size does not need significant changes. Also, increasing the size of clutch plates can negate the advantage of drag at low speeds. After MATLAB calculations, a single-plate clutch with an outer radius of 6.2 cm and an inner radius of 3.6 cm was selected. Figure 9 is obtained by solving the clutch drag torque equation for the number of plates required to transfer the requested torque. As expected, by increasing the number of clutch plates, smaller plates can also be used.

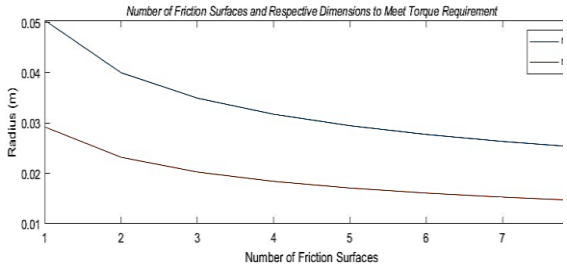

Figure 9. The number and radius size of the clutch plates for the desired torque transmission

The possibility of transferring this amount of torque through the power transmission line, the highest torque and diameter of the gear can be calculated by following equations [18]:

$$T = \frac{\pi D d^2 S_{sy}}{4} \quad (16)$$

$$d = \sqrt{\frac{4T}{D\pi(0.58 S_{sy})}} \quad (17)$$

In summation, the following initial values and assumption are used to start the design and simulation:

- FTP-75 driving cycle is used with a constant slope of 6%, the average frequency of braking to stop from a speed of 60 $\frac{km}{h}$ in a period of 5 seconds with a constant acceleration, the maximum braking power is 28.02 kw (without applying dissipation)

[DOI: 10.22068/ase.2024.671]

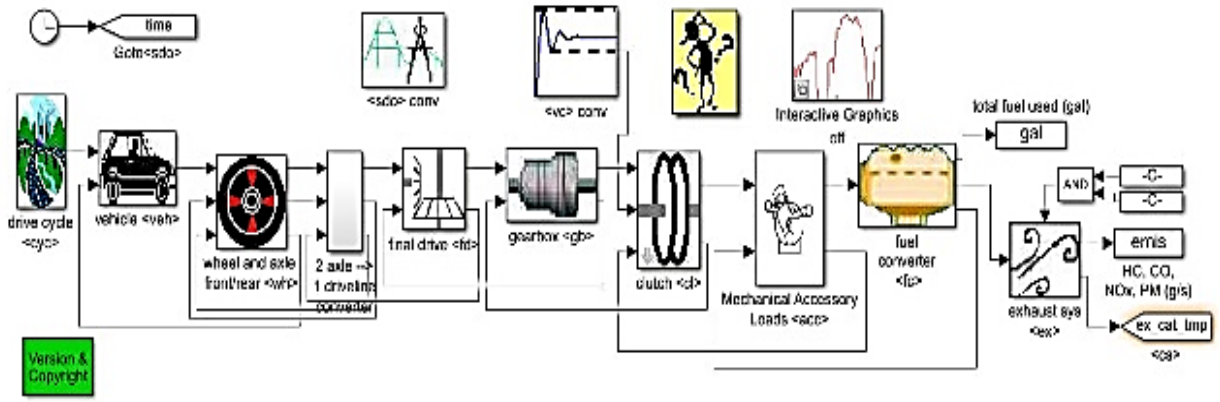

Figure 10. block diagram of advisor simulation for a conventional car

- The mass of the vehicle (Samand) along with the extra weight of the system is about 1500 kg and available energy is 176 kJ for storage (with dissipation).
- Steel flywheel AISI4340 with yield stress of 500 MPa, density of 7800 $^{kg}/_{m^3}$ and Poisson's ratio of 0.3 is selected.
- Incomplete cone flywheel geometry with inner radius 1.95 cm and outer radius 12cm with thickness of 36mm is used.
- Flywheel has a mass of 13 kg and a moment of inertia of 0.19 kg. m^2 with the energy capacity of 183 kJ
- Ratio $\frac{\omega_{min}}{\omega_{max}} = 0.4$ for operating range of flywheel rotation speed.
- The range of CVT speed ratio is 1:8 with a pre-gearing with a speed ratio of 2 and a post-gearing with a speed ratio of 2.5.
- A single plate clutch with 5 cm external radius and 3 cm internal radius, has torque transmission capacity of 22.26 Nm
- A 90% power transmission efficiency, 80% rear axle brake contribution and 1.4 safety factor for flywheel failure are applied.

4. simulation

As shown in Figure 10, a special block is designed for each part of the vehicle power train. This modeling in Simulink determines the contents and data of the blocks by taking the vehicle specifications (such as engine specifications, hybrid type, fuel consumption, gearbox, etc.) and the intended driving cycle. Starting from the driving cycle, and according to that cycle and the driver's decisions, the simulation is performed in Advisor. The final results of this simulation will be the performance of the vehicle in the driving cycle such as the amount of fuel consumption and exhaust emissions.

The simulation is done in both forward/backward methods. There are two types of data, the requested and the available signals, for input and output of each block. The logic of the simulation is that according to the characteristics of the vehicle and the cycle, the calculations of the requested signals are performed in order to reach the final block, i.e. the engine of the vehicle. At this point, the requests are answered from the engine and the available calculations begin. Now the available signals, which are in response to the available requests of the system, are transmitted in the reverse direction of the simulation blocks.

The braking energy recovery system (the mechanical hybrid system) block is added to the differential block. In the conventional vehicles, the differential block (final drive) had two inputs and two outputs. Now, by adding the mechanical kinetic energy recovery system, an input signal (from the flywheel) and an output signal (to the flywheel) were added to the differential block. This add-on is shown in Figure 11.

[DOI: 10.22068/ase.2024.671]

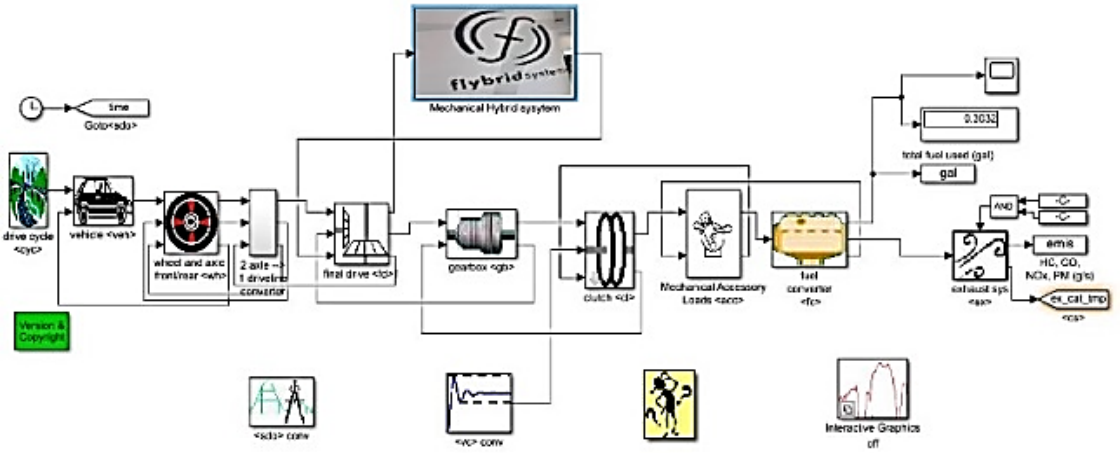

Figure 11. block diagram of advisor simulation for a conventional car

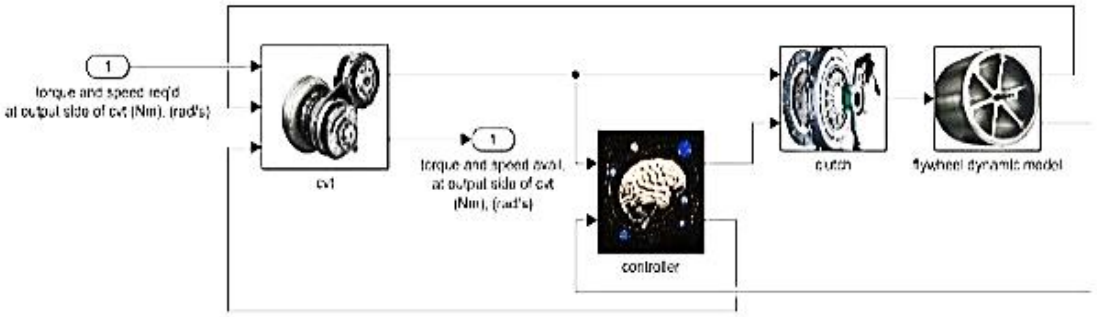

Figure 12. The contents of the mechanical hybrid system block

The requested and available signals of the flywheel are also added to the differential. It takes into account the torque and speed that are available in the energy recovery system and are placed in the priority of the requested signal. As a result, more torque is available (compared to conventional mode) and less requested signal is sent to the engine. The braking energy recovery system with the help of flywheel consists of four sub-assemblies as shown in Figure 12.

1. The flywheel block which includes a moment of inertia. The role of the flywheel as an energy reservoir is due to its inertia:

$$T = I\alpha \tag{18}$$

By having the requested torque from the flywheel and its moment of inertia, the angular acceleration is determined. By integrating the angular acceleration, the available torque and rotational speed of the flywheel are obtained as the output signals of the block. Note that the requested torque sign indicates the state of the vehicle's speed changes and the flywheel connection conditions are always being checked by the controller.

2. The clutch block that acts as binary (zero and one) system. The minimum clutch capacity was calculated during the design phase. According to the conditions checked by the controller (the

[DOI: 10.22068/ase.2024.671]

transmission torque is less than the clutch capacity), the clutch connection status is determined.

3. The CVT and its gearing block that are responsible for converting and transferring torque and speed. Requested torque and speed (which are the signals requested from the differential), available torque and speed (which are the flywheel available signals) as well as the desired CVT ratio (which is determined by the controller) are the three input signals of the CVT block. By multiplying the CVT ratio in the requested speed of the CVT output, the requested speed of the shaft is obtained from the flywheel, which can be used to calculate the torque resulting from the inertia effect and CVT loss. Also, by multiplying the inverse of the CVT ratio in the requested torque of the CVT output and adding it to the torque resulting from the inertia effect and the CVT loss, the requested shaft torque from the flywheel is obtained as the first output.

For the available signal from the flywheel side, the same procedure is used. The only difference is the torque effect from inertia and dissipation (aerodynamic and thermal) is subtracted from the total available torque. Therefore, the available torque signal and speed (which is sent back to the differential) can be obtained as the second output.

The dissipation effect is applied as a fixed torque. Accurate modeling of aerodynamic and thermal losses requires more information (such as pressure, density and temperature inside the chamber air) as well as expertise in the field of fluid mechanics. To obtain this information, modeling of the vacuum chamber in fluid environments is needed. For this reason, in order to maintain the focus of the research on the subject and its purpose, instead of the exact calculation of aerodynamic and thermal losses, simple and approximate modeling has been used.

4. The controller is responsible for checking the existing conditions of the system and design constraints. The torque signal and requested speed from the CVT side and the available speed signal from the flywheel are the inputs of this block. The controller has the task of confirming three statuses in braking and accelerating conditions:

- Checking the speed range of the flywheel.
- Checking the torque transfer request by the clutch with its capacity.
- Checking the range of the CVT ratio (the ratio of the pre and post gears multiplied by the CVT ratio).

These three conditions are necessary to connect the entire flywheel system to the differential. By viewing the state diagram of all three conditions during the cycle as shown in Figure 13, the bottlenecks of the designed system will be revealed. After initial design, the state diagram of three controller conditions was prepared. Status 1 means check (confirmed condition) and 0 means the condition has not been confirmed.

Choosing a material with high strength for the flywheel and increasing its dimensions will increase the capacity of the energy storage (flywheel). The flywheel rotation speed is limited between a minimum and maximum value. The upper limit is caused by stress and the lower limit is caused by the limitation of the range of CVT coefficients. The upper limit is a function of the type and geometry (which is limited due to the available space of the car and economic considerations) and the lower limit is a function of the type of CVT and the pre and post gearing. By choosing a CVT with a wider ratio range (like IVT) and finding the optimal pre and post gear ratios the energy storage capacity (flywheel) is more utilized.

An optimal system is one that has a three-condition state diagram with maximum overlap. According to the Figure 13, it is clear that the flywheel speed range condition, creates the least constraint for the system. The frequency of changing the state of the condition of clutch capacity is higher than the other two conditions. It means that a small clutch capacity is considered for the initial values and as soon as the system is connected, the clutch capacity is filled. In the next level, the range of CVT ratios prevents the utilization of the flywheel capacity.

[DOI: 10.22068/ase.2024.671]

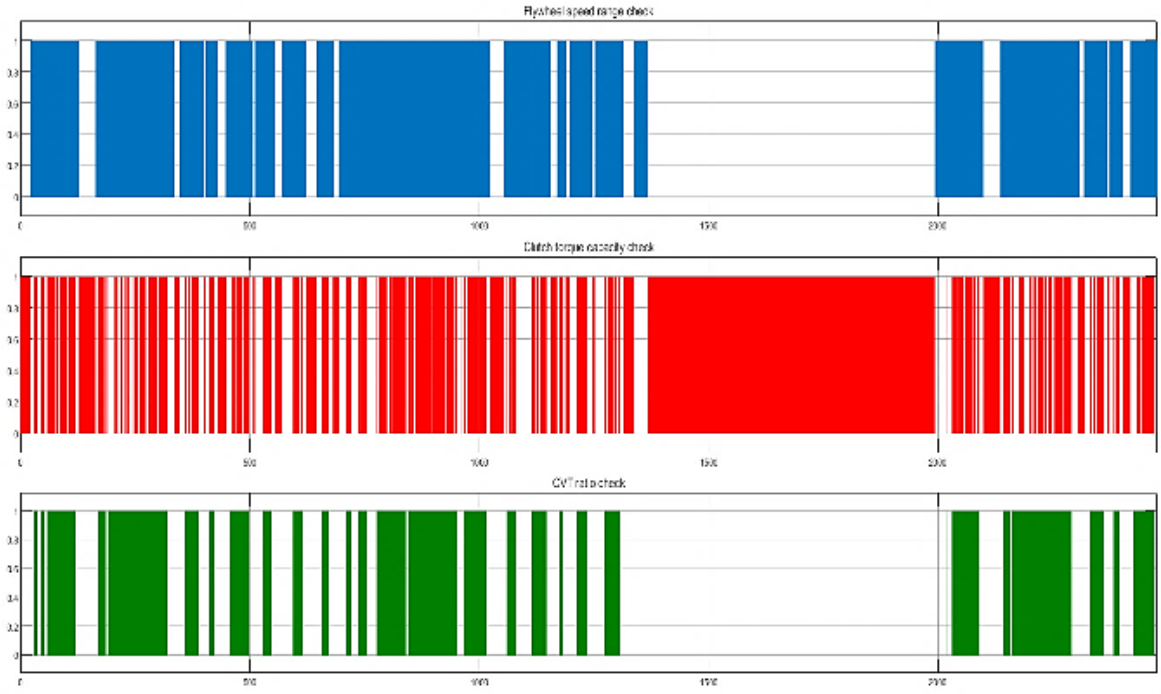

Figure 13. Status of controller conditions for design initialization

Condition diagram analysis provides a comprehensive view of system bottlenecks.

Connection conditions and control policy of the system vary depending on the design purpose. The purpose of designing this system is to reduce the fuel consumption as much as possible for typical conventional vehicles. In some cases (such as Formula One racing cars), the design policy and purpose of this system is simply to recover braking energy and use it for greater acceleration. Keep in mind that the basis of the design is based on the assumptions and the output is obtained as a function of them. By changing any assumption, the output can change a lot. In the following, some of the initial design assumptions and values that caused the bottleneck have been mentioned and solutions have been provided. In the “CVT ratio" section of the control block, dividing the flywheel speed by the differential speed, a diagram of the requested ratios of the pre, post gears and CVT is obtained and shown in Figure 14.

The requested ratios diagram tends toward infinity in many cases. Also, between the minimum value and the ratio of 100 has the highest occurrence. This minimum value depends on the type of engine, gearbox and driving cycle. Based on the power transmission components from the differential to the flywheel and the requested ratio chart, the components of the power transmission system can be selected. Therefore, the minimum value as the ratio of the pre gear is selected and the condensed area is set for the entire transmission ratio range.

[DOI: 10.22068/ase.2024.671]

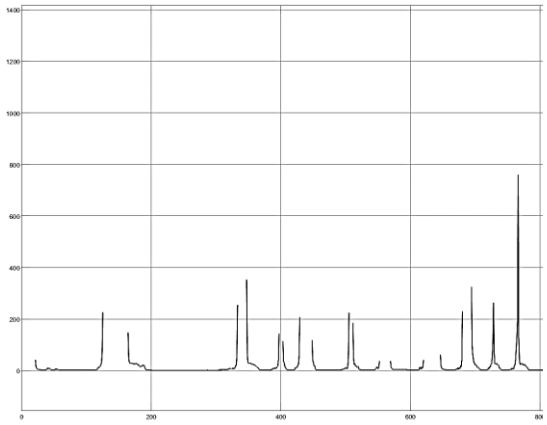

Figure 14. Diagram of requested ratios of the power transmission system

Table 2. The impact of changes ω_{min} on system performance

ω_{min} (rad/s)	ω_{max} (rad/s)	Safety factor $(\frac{1783}{\omega_{max}})$	Fuel reduction (%)
100	1783	1	4.77
300	1566	1.14	6.62
500	1261	1.41	11.47
700	1340	1.33	10.1
891.5	1435	1.24	8.54
1000	1297	1.37	12.75
1200	1653	1.08	5.06

5. Results and validation

The result of the simulation with the initial values showed 6% fuel consumption reduction. It was also observed that the minimum capacity for the clutch is the bottleneck of the system. Therefore, the Samand's original clutch is used which provides the torque transmission capacity of 150N.m. With this clutch capacity, the CVT ratio range is 1:8, the pre gear with a ratio of 2 and the post gear with a ratio of 2.5 (in total, the ratio range is 2:40 for the entire power transmission system) was selected. In order to better understand the effect of changing the initial assumptions and also validation of the results, in the following sections, the flywheel performance under different values for Flywheel's speed range, CVT, and Clutch capacities are evaluated.

5.1. Effect of flywheel speed range

Results of the first test is given in Table 2. The effect of changing the minimum allowable speed of the flywheel is considered, and the rest of the values are unchanged. The maximum allowable rotation speed of the flywheel is 1783 rad/s and the moment of inertia 0.19 kg. m^2.

Note that the maximum permissible rotational speed of the flywheel depends on the material and geometry. For the flywheel with the desired specifications, this speed is fixed and cannot be exceeded.

For constant power to be transmitted by the clutch, the lower the rotational speed, the greater the torque. As a result, after analyzing the connection conditions by the controller, the clutch is known as the limiter of the system. Also, by increasing the permissible flywheel rotation speed range (that is, reducing the minimum flywheel speed), the CVT will not be able to satisfy the low ratios. Thus, the limiting factor for very high and low speeds will be the CVT.

The minimum operating speed of the flywheel suggested by most studies (such as [20]) is half of the maximum allowed speed. This is not always correct and to some extent it can be a suitable option. But to find a more optimal answer, it is necessary to know the impact of other design assumptions on the system performance. According to the reliability of the considered system, a flywheel with a lower moment of inertia can be used. By reducing the size or changing the material of the flywheel to a lighter material, the manufacturing cost, volume and weight can be reduced and, as a result, the efficiency of the

[DOI: 10.22068/ase.2024.671]

design can be increased. Providing minimum flywheel speed is critical. Because when starting to drive, the flywheel is stopped, so the speed of the flywheel is not within the allowed range, and the ratio of the speed of the differential to the flywheel tends to infinity. As a result, the connection conditions will never be established by the controller and it will not be charged. Ensuring the minimum speed of the flywheel can be done in different ways. In some cases, it is provided by a small motor that is powered by an alternator and is installed in the center of the flywheel disk. In mechanical cases, this minimum speed is provided by the differential. Providing this minimum speed is not very expensive if it is not high. Increasing the minimum speed not only increases the cost of providing it, but also reduces the performance and reliability of the system in some cases. Therefore, the design is preferred over the minimum speed capability.

5.2. The effect of increasing CVT capacity

The second test investigates the effect of increasing the range of CVT coefficients which was used in the first test and caused operational limitations (other assumed values are constant). In the second test, the speed ratio range was changed to 2:50 and the results are shown in the Table 3.

Table 3. Increasing the range of CVT ratios to 2:50

ω_{min} (rad/s)	ω_{max} (rad/s)	Safety factor $(\frac{1783}{\omega_{max}})$	Fuel reduction (%)
100	1783	1	7.75
200	1783	1	8.73
300	1721	1.03	7.45
400	1684	0.06	9.23
500	1290	1.38	11.72

Examining the graph of Figure 14, the requested ratio of the CVT shows two important points:

- The minimum required coefficient of the considered CVT with pre and post gearing is 4.25
- The graph tends to infinity at many points and has the highest density up to a ratio of 100.

For this reason, the range of speed ratios can be increased to 4:100 and corresponding results are shown in Table 4.

Table 4. Increasing the range of CVT ratios to 4:100

ω_{min} (rad/s)	ω_{max} (rad/s)	Safety factor $(\frac{1783}{\omega_{max}})$	Fuel reduction (%)
100	1421	1.07	2.98
200	1352	1.32	6.86
300	1266	1	7.68
400	1320	1.43	7.92
500	1345	7.2	9.65

Contrary to expectations, except for one case, by increasing the capacity of the power transmission system (increasing the CVT speed ratio range of 4:100), an increase in fuel consumption was resulted for all other cases, as compared to the previous state. This did not occur for the speed ratio range to 2:50.

5.3. The effect of increasing clutch capacity

The effect of increasing clutch capacity was investigated as the third test. For the speed ratio range of 2:50, the clutch capacity increased from 150 Nm to 200 and 300 Nm as presented in Tables 5 and 6 respectively.

[DOI: 10.22068/ase.2024.671]

Table 5. Increasing clutch capacity to 200 Nm

ω_{min} (rad/s)	ω_{max} (rad/s)	**Safety factor** ($\frac{1783}{\omega_{max}}$)	**Fuel reduction** (%)
100	1783	1	5.43
200	1783	1	7.51
300	1721	1.08	8.58
400	1684	1.4	9.67
500	1290	1.38	10.1

Table 6. Increasing clutch capacity to 300 Nm

ω_{min} (rad/s)	ω_{max} (rad/s)	**Safety factor** ($\frac{1783}{\omega_{max}}$)	**Fuel reduction** (%)
100	1783	1	6.12
200	1783	1	7.65
300	1783	1	7.89
400	1270	1.4	7.71
500	1239	1.43	11.53

Contrary to expectations, in some cases, the results of increasing the clutch capacity also show an increase in fuel consumption as compared to the previous state. The intention of increasing the capacity of the system (clutch or CVT) was to further reduce fuel consumption, and it was expected that by increasing the capacity of the clutch, the ability to transfer the torque through the system would increase. Also, by increasing the range of CVT coefficients, the range of flywheel operation speed will increase. But this idea does not hold always for vehicles, and the answer to this divergence of results lies in the engine fuel consumption map.

5.4. Divergent results

A typical engine fuel consumption map is shown in Figure 15. This diagram consists of different contours that shows the fuel consumption for each engine speed and torque. According to this map, for each requested engine speed and torque, there are optimal points with the lowest fuel consumption, which show the optimal points of the engine's performance. The closer the engine operating points are to the center of the map, the lower the fuel consumption. When the connection conditions are established, the clutch connects the flywheel to the differential and the whole set is spinning as one. Now, with the addition of the energy recovery system, at a certain speed of the differential, the request torque from the engine is reduced. As it can be seen in Figure 15, by reducing the requested torque from the engine at a certain speed (moving from point A to B), shows the divergence in the above results at a specific moment of the driving cycle.

[DOI: 10.22068/ase.2024.671]

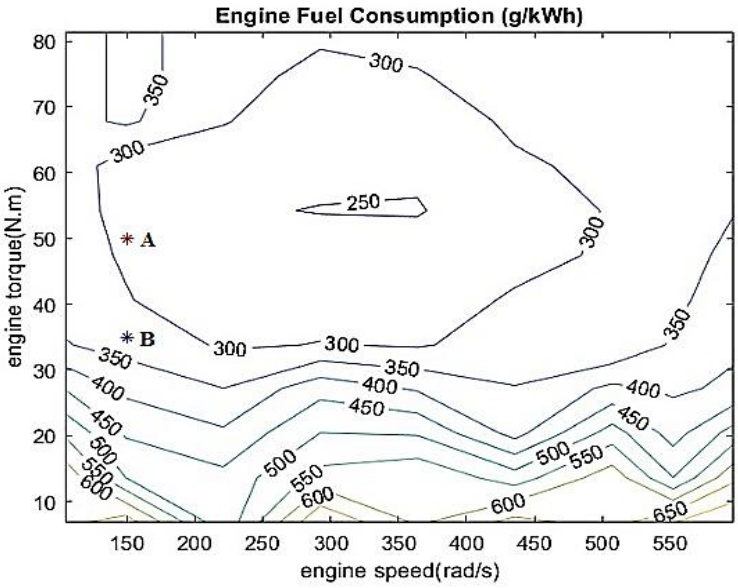

Figure 15. Map of engine hard consumption at two points of divergence from the results

Two solutions to this problem can be proposed:

1. Optimizing design values to avoid over design capacity of the system and divergent results. According to this scenario, some system bottlenecks (described in the connection condition control diagram) inevitably cannot be resolved, because it may have the opposite effect on the system.

2. Upgrading the controller level by adding new conditions to the rational of the control system. For instance, taking into account the engine operating points at any speed in making connection decision. In this case, the fourth condition will be added to the connection conditions and the bottleneck analysis of the system will be completely transformed. Upgrading the controller level does not mean optimization and will simply make more correct decisions for system connectivity.

6. Discussion

In the present study, a proper kinetic energy recovery system (KERS) for Samand passenger car was designed. Initially, theorical model of the KERS system was developed examining previous studies and successful implementations by major automotive companies. It then proceeded to design the components of a KERS tailored to this particular vehicle, establishing the necessary scale and minimum requirements. To evaluate the design's performance and the impact of various assumptions, simulations were conducted using Simulink. The analysis highlighted how different design assumptions influenced the system's efficiency and diverging results. The simulation and design efforts demonstrated that achieving a 12% reduction in fuel consumption for a vehicle with the characteristics of the Samand is feasible under the considered driving cycle. However, the optimization process for the simulation was not exhaustive, suggesting that further fuel consumption reductions are possible. Existing prototypes also support this potential.

Research on flywheel-based kinetic energy recovery systems often integrates generators and batteries. Studies focusing on purely mechanical models of these systems are rare and typically

[DOI: 10.22068/ase.2024.671]

compare this hybridization model with other models, providing theoretical calculations to support their claims. The novelty of this research lies in the comprehensive simulation of a flywheel-based braking energy recovery system using Simulink, utilizing the Advisor add-on for a more realistic model. Additionally, the discussion on factors affecting system efficiency, especially the divergent results that contradict the claims of many sources, contributes to the innovation of this study.

7. Conclusion

This thesis began with a comprehensive review of kinetic energy recovery systems (KERS), examining successful implementations by major automotive manufacturers. The primary focus was on developing a KERS prototype compatible with the Samand car, employing a flywheel tank as the energy storage mechanism. The design considerations included the type and dimensions of the power transmission system and clutch, which were carefully selected based on various influencing factors. Initial designs were simulated and evaluated using MATLAB_SIMULINK and the ADVISOR plugin to assess their performance. The simulations focused on understanding the impact of different design parameters on system efficiency. The results indicated that a 12% reduction in fuel consumption for the Samand car could be achieved during urban driving cycles characterized by frequent braking. This improvement was attributed to the use of a steel flywheel with an incomplete cone geometry and a specific radius. The study highlighted several areas for further development and improvement:

1. **Controller Enhancement:** Modifying flywheel geometry and material, adjusting gear ratios and CVT, increasing clutch capacity, and optimizing the flywheel speed range based on engine performance can enhance system efficiency. Each simulation assumption significantly impacts the results, highlighting the need for expertise in optimization algorithms to further reduce fuel consumption.

2. **Design Objective Shift:** For race cars, braking energy recovery systems should focus on enhancing speed and acceleration rather than fuel efficiency. This requires different control strategies and energy release methods.

3. **Precise Loss Simulation:** Modeling aerodynamic and thermal losses of the flywheel in a variable pressure chamber can help understand and optimize these factors, potentially reducing production and consumption costs.

4. **Electrical Hybridization:** Combining flywheel energy storage with battery and generator systems can address the weaknesses of each, providing improved performance. This hybrid approach can be applied to various devices with variable kinetic energy, beyond just vehicles.

5. **Stability Analysis:** Stability is crucial for any control system. Future research should involve mathematical modeling and simulation to analyze stability, ensuring the system's response to disturbances remains controlled over time.

Overall, this study demonstrates the viability of mechanical KERS as a complement or alternative to hybrid models involving batteries and generators. The insights and recommendations provided pave the way for future research and development, aiming to optimize fuel efficiency and enhance the performance of kinetic energy recovery systems in vehicles. The findings also suggest a significant potential for reducing emissions and improving the environmental friendliness of vehicles equipped with such systems.

Declaration of Conflicting Interests

The author(s) declared no potential conflicts of interest with respect to the research, authorship, and/or publication of this article.

References

[1] Shafiee S., Topal E., When will fossil fuel reserves be diminished?, Energy policy, (2009), 37(1):181-9.

[2] Li, X., & Palazzolo, A, A review of flywheel energy storage systems: state of the art and

[DOI: 10.22068/ase.2024.671]

opportunities, Journal of Energy Storage, (2022), 46, 103576.

[3] Dimitrova, Z., & Maréchal, F., Gasoline hybrid pneumatic engine for efficient vehicle powertrain hybridization., Applied Energy, (2015), 151, 168-177.

[4] Midgley WJ., Cebon D., Comparison of regenerative braking technologies for heavy goods vehicles in urban environments, Proceedings of the Institution of Mechanical Engineers, Part D: Journal of Automobile Engineering, (2012), 226(7):957-70.

[5] Boretti, A, Comparison of fuel economies of high efficiency diesel and hydrogen engines powering a compact car with a flywheel based kinetic energy recovery systems, International Journal of Hydrogen Energy, (2010), 35(16), 8417-8424.

[6] Gunatilake, W.A.D.N., Herath, B.G.H.M.M.B., Bowatta, B.G.C.T., Jayaweera, N.D. and De Silva, C.M.S.P., Design and development of kinetic energy recovery system for motor vehicles, University of Moratuwa, Sri Lanka, (2015).

[7] Śliwiński C., Kinetic energy recovery systems in motor vehicles, InIOP Conference Series: Materials Science and Engineering, (2016), Sep 1 (Vol. 148, No. 1, p. 012056), IOP Publishing.

[8] Rakov V., Determination of optimal characteristics of braking energy recovery system in vehicles operating in urban conditions, Transportation Research Procedia, (2020), Jan 1;50:566-73.

[9] https://www.epa.gov/emission-standards-reference-guide/epa-federal-test-procedure-ftp, May 2024.

[10] Dhand A, Pullen K., Review of flywheel based internal combustion engine hybrid vehicles, International Journal of Automotive Technology, (2013), 14(5):797-804.

[11] Skinner, M., & Mertiny, P., Energy Storage Flywheel Rotors—Mechanical Design, Encyclopedia, (2022), 2(1), 301-324.

[12] Eltaweel, M, Herfatmanesh, M. R., Enhancing vehicular performance with flywheel energy storage systems: Emerging technologies and applications, Journal of Energy Storage, (2024), Volume 103, Part B, 114386.

[13] Thoolen FJ., Development of an advanced high-speed flywheel energy storage system, (1993).

[14] Purohit K., Sharma C., Design of Machine Elements: PHI Learning Pvt. Ltd., (2002).

[15] Arslan MA., Flywheel geometry design for improved energy storage using finite element analysis, Materials & Design, (2008), 29(2):514-8.

[16] Lawson LJ., Design and testing of high energy density flywheels for application to flywheel/heat engine hybrid vehicle drives., InIntersociety Energy Conversion Engineering Conference, (1971), Aug (pp. 1142-1150).

[17] Vander Voort, G. F., Lampman, S. R., Sanders, B. R., Anton, G. J., Polakowski, C., Kinson, J., ... & Scott Jr, W. W., "Metallography and microstructures", ASM handbook, (2004), 9, 44073-0002.

[18] Juvinall RC, Marshek KM., Fundamentals of machine component design., John Wiley & Sons, (2020), Jun 23.

[19] Kodaganti Venu MK. Wet clutch modeling techniques - Design optimization of clutches in an automatic transmission (Master thesis), Department of Applied Mechanics, Chalmers University Of Technology, (2013).

[DOI: 10.22068/ase.2024.671]